

Synergistic anti-proliferative activities of 10-hydroxy-2-decenoic acid in adjunct to doxorubicin in MCF-7 breast cancer cells

Wantha Jenkhetkan^a, Arunporn Itharat^b, Supranee Kongkham^c, Srisopa Ruangnoo^b, Treetip Ratanavalachai^{c,*}

^a Division of Biochemistry and Molecular Biology, Faculty of Medicine, Thammasat University, Pathum Thani 12120 Thailand

^b Department of Thai Traditional Medicine, Faculty of Medicine, Thammasat University, Pathum Thani 12120 Thailand

^c Department of Preclinical Sciences, Division of Biochemistry, Faculty of Medicine, Thammasat University, Pathum Thani 12120 Thailand

*Corresponding author, e-mail: treetip2000@gmail.com

Received 7 Jan 2021
Accepted 14 Sep 2021

ABSTRACT: Among all cancers, the global incidence rate of breast cancer is the highest. Novel chemotherapeutic agents are needed to improve the existing chemotherapy outcomes and to reduce the toxic side effects. 10-hydroxy-2-decenoic acid (10-H2DA), a royal jelly acid, had been reported to have anti-inflammatory, anti-tumor, and anti-metastasis activities. This study aimed to investigate anti-proliferative efficacy and the underlying mechanisms of 10-H2DA co-treatment with doxorubicin (DXR), a chemotherapeutic compound, in MCF-7 breast cancer cells. MTS assay was conducted to determine cell viability. Cell cycle progression and cell apoptosis were detected by flow cytometry. Pivotal protein expressions were determined by Western blot. Results revealed that the 125 µg/ml 10-H2DA co-treatment with the 0.54 µg/ml DXR synergistically and significantly inhibited cancer cell growth up to 79%, compared with the medium control ($p < 0.05$); it was 1.6-fold higher than the DXR treatment alone. The underlying mechanisms involved extensive suppression of oncoprotein c-MYC/BAX and activation of tumor suppressor The two mechanisms led to G1/S cell cycle arrest, cell apoptosis, and shortened lifespan. The activations of HO-1/BAX and p53/BAX while suppressing NRF2/BAX expression suggested induction of cell ferroptosis. Our findings suggest that the 10-H2DA in adjunct to the DXR is a promising novel candidate for breast cancer treatment via extensive decrease in C-MYC/BAX, increase in p53/BAX, cell cycle arrest, and cell apoptosis. Further *in vivo* mechanistic studies are necessary to validate its benefits.

KEYWORDS: antiproliferation, apoptosis, doxorubicin, 10-hydroxy-2-decenoic acid, cell cycle arrest, c-MYC

INTRODUCTION

The age-standardized (world) incidence rate of breast cancer is the highest among all cancers (37.8 per 100 000), and breast cancer is the third leading cause of death (age-standardized mortality rate: 12.7 per 100 000) [1]. More effective cancer treatments are still needed. Chemotherapy is commonly used to treat breast cancer in combination with other tools such as surgery, radiotherapy, and hormonal therapy. However, most chemotherapeutic agents have limitations on their potency due to induction of toxic side effects and drug resistance [2]. For example, doxorubicin (DXR), an anthracycline, inhibits DNA topoisomerase II and generates free radicals to kill cancer cells; however, it induces drug resistance and cardiovascular toxicities (cardiomyopathy and congestive heart failure) [3, 4]. Cisplatin (CDDP), a metallic (platinum) coordination compound, binds to DNA and inhibits DNA replication and DNA repair; it also induces nephrotoxicity and drug resistance [5]. It has been reported that using natural bioactive compounds in adjunct to chemotherapeutic agents enhances ther-

apeutic potentials and limits drug resistance [6]. 10-hydroxy-2-decenoic acid (10-H2DA), the most abundant fatty acid in royal jelly, has been reported to have various pharmacological properties such as anti-aging [7], anti-inflammatory [8], anti-bacterial [9], and anti-tumor [10]. Besides, it completely inhibited the tumor development of transplantable leukemia and ascites tumor cells in mice [10, 11]. It also inhibited VEGF-induced angiogenesis, tumor cell invasion, and metastasis in aggressive chemoresistant breast cancer cells [12]. 10-H2DA strongly inhibited nitric oxide and inflammatory-related cytokines in lipopolysaccharide-stimulated RAW264.7 macrophages cells [8].

Our previous studies [13] revealed that the 10-H2DA treatments (1.25, 12.5, and 125 µg/ml) significantly inhibited MCF-7 cell proliferation. The 125 µg/ml 10-H2DA treatment maximally decreased the MCF-7 breast cancer cell viability to 34.6% compared with the medium control and 1.4-fold better than the 0.54 µg/ml DXR treatment. The 50% inhibition concentration (IC₅₀) value derived from the log[10-H2DA] scale was 42.6 µg/ml. The inhibitory mechanisms involved extensive suppression of cell pro-

liferation via decreased c-MYC/BAX, shortened lifespan, and induced cell apoptosis. However, it increased anti-oxidative power by increasing the NRF2/BAX and the HO-1/BAX, possibly inducing cancer cell resistance.

We then hypothesized that the 10-H2DA in adjunct to the DXR would synergistically inhibit breast cancer cell proliferation. To verify our hypothesis, we investigated the anti-proliferative activities and the underlying molecular mechanisms of the 10-H2DA co-treatments with the DXR in MCF-7 breast cancer cells. Cell viability, cell cycle progression, cell apoptosis, and pivotal protein expressions were determined. Results demonstrated that the 10-H2DA co-treatment with the DXR at proper doses strongly inhibited breast cancer cell growth via systemic modulation of pivotal regulatory proteins. The co-treatment successfully induced cell apoptosis, cell cycle arrest, limited lifespan extension, and possibly limited cancer cell resistance.

MATERIALS AND METHODS

Cancer cell line and chemicals

Epithelial breast adenocarcinoma cell line, MCF-7 (HB22), was purchased from American Type Culture Collection (ATCC), USA. 10-hydroxy-2-decenoic acid was purchased from Cayman Chemical Company, USA: CAS No. 14113-05-4, 98% purity. Doxorubicin hydrochloride (Adriamycin) was purchased from Pfizer, USA.

Determination of anti-proliferative activities by MTS tetrazolium assay

The MCF-7 cells were cultured in MEM medium with supplements at 37 °C in a 5% CO₂ incubator for 24 h according to the manufacturer's protocol. Cells were then co-treated with 10-H2DA (0.0125, 0.125, 1.25, 12.5, and 125 µg/ml) and 0.54 µg/ml (1 µM) DXR for 24 h. MEM medium and DXR alone were used as negative and positive controls, respectively. The IC50 value was determined using GraphPad Prism7 via log scale.

Analysis of cell cycle distribution and cell apoptosis by flow cytometry

To determine cell cycle distribution, the treated MCF-7 cells were washed and fixed with 70% cold ethanol overnight at -20 °C. Cells were then stained with propidium iodide (PI)/ribonuclease staining buffer (BD Biosciences, USA) for 20 min at room temperature. The cell cycle distribution was measured with Guava EasyCyte™ Flow Cytometer (Merck Millipore, USA) using GuavaSoft software.

Annexin V-FITC apoptosis detection kit I (BD Biosciences, USA) was applied to detect cell apoptosis. The treated cells were washed and incubated with FITC Annexin V and PI for 15 min in the dark at room temperature. The cells were analyzed immediately by

Guava EasyCyte™ Flow Cytometer (Merck Millipore, USA).

Nuclear morphological changes detected by Hoechst33258/Propidium iodide double staining

The treated MCF-7 cells were washed and stained with 10 µg/ml Hoechst 33258 solution for 7 min at 37 °C in a CO₂ incubator. The cells were then counterstained with propidium iodide (PI) (2.5 µg/ml) for 15 min in the dark at room temperature. The stained cells were immediately analyzed under a fluorescence microscope. The Hoechst 33258 stained DNA in dark blue and cells with apoptotic nuclei in bright blue, whereas the PI counterstained DNA of the dead cells in red. When merged, the dead cells with apoptotic nuclei showed double staining colors of bright blue with red apoptotic nuclei.

Analysis of pivotal protein expressions using Western blot

The treated cells were lysed and boiled with RIPA lysis buffer (Merck Millipore, USA). The lysate was separated using 10% SDS-polyacrylamide gel electrophoresis, followed by blotting onto a nitrocellulose membrane (GE Healthcare, USA), and blocked with Odyssey blocking buffer (LI-COR, USA). Membranes were then probed with corresponding rabbit primary antibodies: anti-hTERT, anti-HO-1, anti-NRF2, anti-cyclin D1, and anti-cyclin D (Merck Millipore, USA); and anti-c-MYC, anti-p53, anti-BCL2, anti-BAX, anti-cyclin B1, anti-cyclin E1, and anti-CDK4 (Cell Signaling, USA). Anti-β-actin polyclonal antibody (Cell Signaling, USA) was used as an internal control. After that, membranes were washed and incubated with LI-COR IRDye 680 mouse anti-rabbit. The protein bands were visualized using Odyssey FcImager (LI-COR, USA).

RESULTS AND DISCUSSION

Antiproliferative activity detected by MTS assay

All 10-H2DA co-treatments: 0.125, 1.25, 12.5, and 125 µg/ml with 0.54 µg/ml DXR for 24 h significantly decreased MCF-7 cell viability in a dose-dependent manner to 73%, 71%, 51%, and 27.9%, compared with the medium control ($p < 0.05$), respectively (Fig. 1a). The IC50 value derived from the log scale was 13.6 µg/ml (Fig. 1b). The DXR treatment alone significantly decreased cell viability to 52%. Since the 125 µg/ml 10-H2DA treatment alone significantly decreased cell viability to 34.6% [13]; therefore, 125 µg/ml 10-H2DA treatment in combination with the DXR synergistically inhibited cancer cell growth (1.5-fold, compared with the DXR treatment alone). However, the low doses of 0.0125, 0.125, and 1.25 µg/ml 10-H2DA co-treatments tended to have antagonistic effects. The percentages of the cell viabilities were ~1.4 times higher than that of the DXR

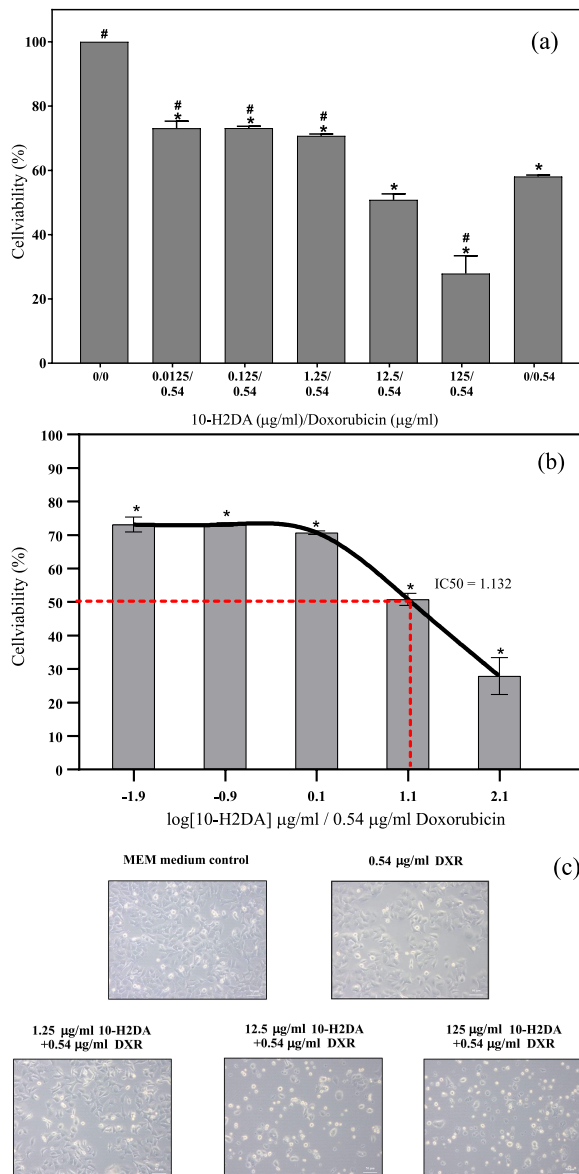


Fig. 1 (a) Effects on cell proliferation induced by various concentrations of the 10-H2DA co-treatments with DXR on MCF-7 breast cancer cells ($n = 3$); ** $p < 0.05$ significantly different from the MEM medium control (without 10-H2DA and DXR); # $p < 0.05$ significantly different from the DXR; (b) determination of IC₅₀ value in log scale; (c) effects of the MEM medium control (0), the 10-H2DA-DXR co-treatments, and the DXR treatment alone on cell morphology.

treatment alone. The inhibitory efficacy of 10-H2DA was dose dependent. Cell morphology after treatments demonstrated under a light microscope showed that the higher doses of the 10-H2DA co-treatments and the DXR treatment resulted in more toxic cells with unattached and rounded shapes (Fig. 1c).

Effects on cell cycle progression detected by flow cytometry

Compared with the MEM medium control, the 125 μg/ml 10-H2DA co-treatment with 0.54 μg/ml DXR significantly increased the percentage of cells in the sub G1 phase (30-fold), (Fig. 2a and 2b) while decreasing the percentages of cells in G0/G1 (0.6-fold), S (0.5-fold), and G2/M (0.8-fold) phases. It demonstrated that the 125 μg/ml 10-H2DA co-treatment maximally induced cell apoptosis and limited cell cycle progression. The DXR treatment alone increased the percentage of cells in the sub G1 phase (6.7-fold), suggesting induction of cell apoptosis. Besides, it decreased the percentages of cells in G0/G1 (0.8-fold) and S (0.5-fold) phases but increased in G2/M (1.2-fold) phase, indicating induction of G2/M cell cycle arrest. The low dose of 1.25 μg/ml 10-H2DA co-treatment decreased the percentages of cells in G0/G1 (0.8-fold) and S (0.6-fold) phases but increased in G2/M (1.2-fold) and sub G1 (3.8-fold) phases. Results showed that both 1.25 μg/ml 10-H2DA co-treatment and the DXR treatment alone induced G2/M cell cycle arrest. The co-treatment, however, induced slightly less cell apoptosis.

Effects on cell cycle regulatory proteins detected by Western blot analyses

As shown in Fig. 3a and 3b, the 10-H2DA co-treatments (1.25, 12.5, and 125 μg/ml) with DXR decreased the CDK4 and the cyclin D1 in a dose-dependent manner, compared with the MEM medium control. In addition, the 125 μg/ml 10-H2DA co-treatment maximally decreased the CDK4 (0.3-fold) and the cyclin D1 (0.5-fold). Contrarily, it increased the cyclin E1 (2.1-fold) and the cyclin B1 (1.5-fold). The data verified that the 125 μg/ml 10-H2DA co-treatment induced the G0/G1 cell cycle arrest (with decreased CDK4 and cyclin D1). The DXR treatment alone decreased the levels of the cyclin B1 (0.4-fold) while increasing the cyclin E1 (2.5 fold) and the cyclin D1 (1.2 fold), signifying the G2/M cell cycle arrest. The 1.25 μg/ml 10-H2DA co-treatment decreased the cyclin B1 (0.5-fold) and slightly decreased the CDK4 (0.7-fold) and the cyclin D1 (0.9-fold) while maximally increasing the cyclin E1 (3.8-fold). This low dose of the 10-H2DA co-treatment induced the G2/M arrest, similar to the DXR treatment alone. Results from Western blot analyses of cell cycle regulatory proteins were in agreement with results from cell cycle analyses detected by flow cytometry.

Effects on cell apoptosis of 10-H2DA co-treatments detected by flow cytometry

Compared with the MEM medium control, the 10-H2DA co-treatments of 1.25, 12.5, and 125 μg/ml with the DXR markedly induced a dose-dependent increase in the percentages of early apoptotic cells to 1.6-, 2.6-

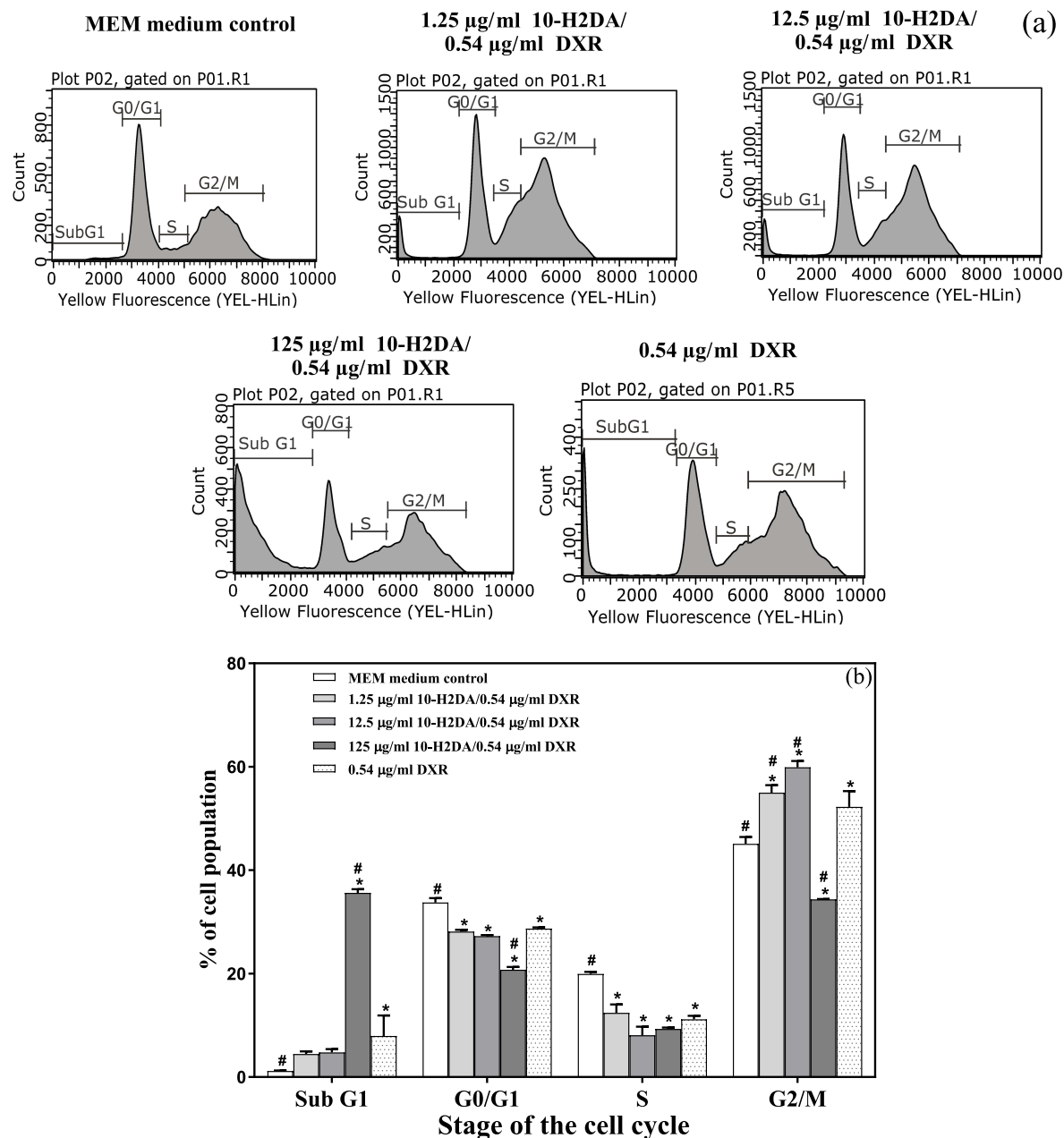


Fig. 2 (a) Cell cycle analyses of MCF-7 cells after various concentrations of the 10-H2DA co-treatments with 0.54 µg/ml DXR for 24 h. The MEM medium and the DXR were used as negative and positive controls ($n = 3$). (b) Percentages of the cell population in individual stage of the cell cycle after treatments (mean \pm SE); * $p < 0.05$ significantly different from medium control; # $p < 0.05$ significantly different from the DXR.

, and 4.9-fold; but slightly increased the percentages of late apoptotic/necrotic cells to 1.2-, 1.1-, and 1.1-fold, respectively (Fig. 4a and 4b). The DXR treatment alone increased the percentage of early apoptotic cells (2.4-fold) while slightly decreasing the percentage of late apoptotic/necrotic cells (0.9-fold). The results demonstrated that the highest 125 µg/ml 10-H2DA co-treatment effectively increased the percentage of

early apoptotic cells the most, twice as much as that of the DXR treatment alone. However, the 1.25 µg/ml 10-H2DA co-treatment decreased percentage of early apoptotic cells, compared with the DXR treatment alone (1.5-fold decrease) while slightly increasing percentage of late apoptosis (1.2-fold). Therefore, the low dose of 1.25 µg/ml 10-H2DA co-treatment reduced the DXR-induced cell apoptosis.

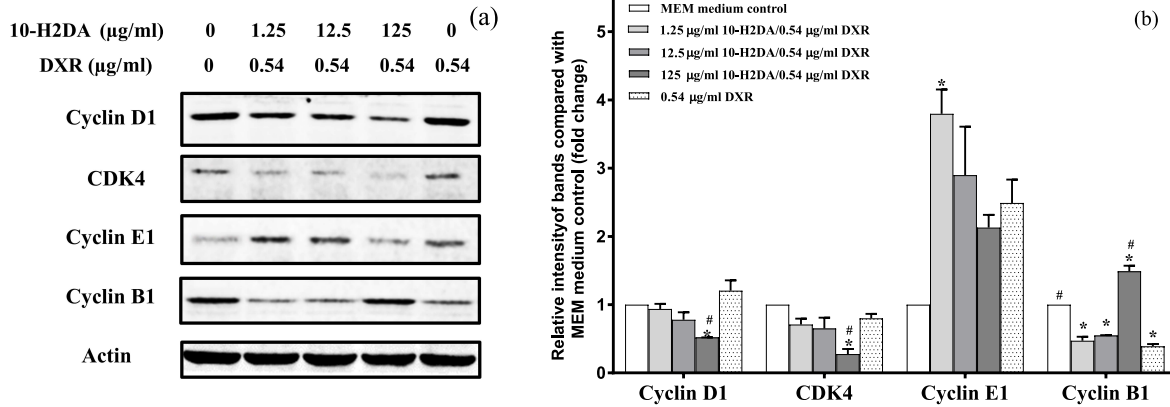


Fig. 3 (a) Representative Western blot analyses induced by various concentrations of the 10-H2DA co-treatments with DXR in MCF-7 cells; (b) relative intensities of bands compared with the MEM medium control ($n = 3$); * $p < 0.05$ significantly different from the medium; # $p < 0.05$ significantly different from the DXR.

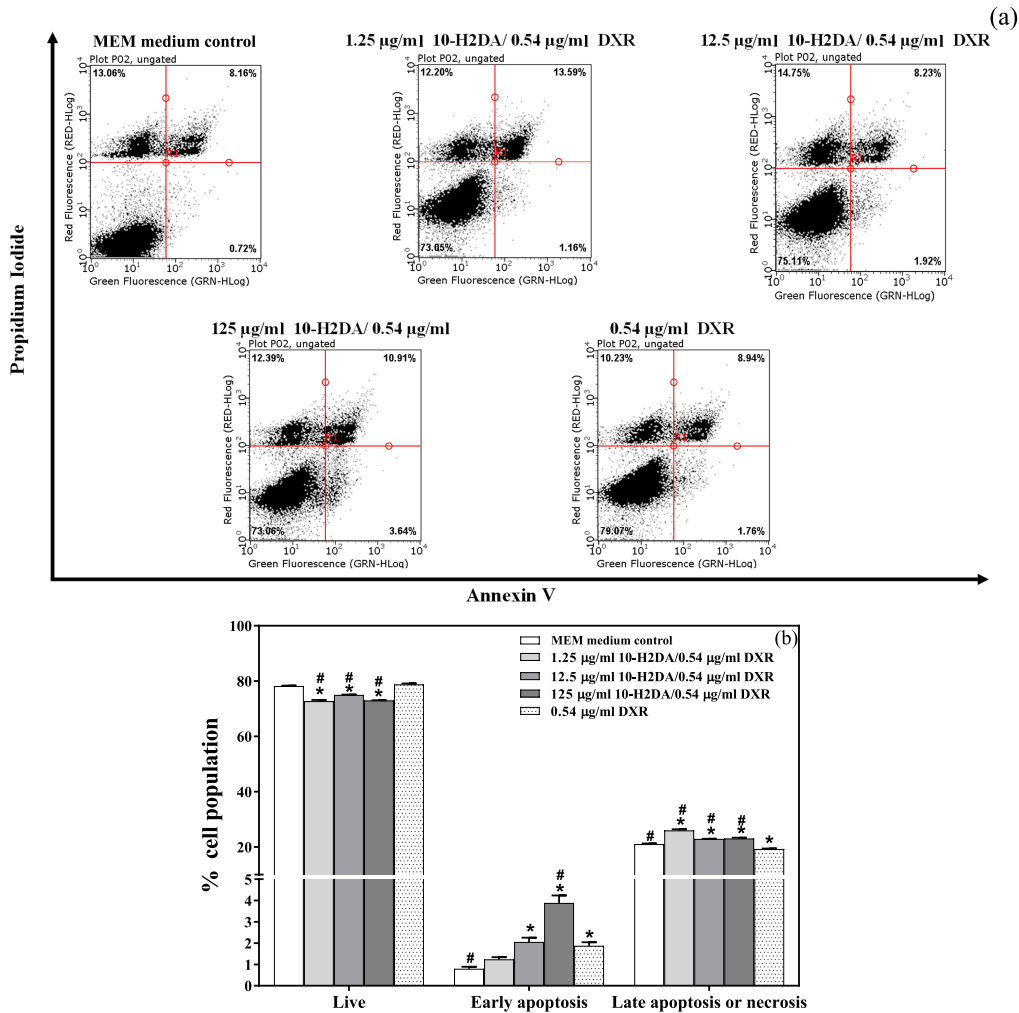


Fig. 4 (a) Representative apoptosis diagram of MCF-7 cells exposed to various concentrations of 10H2DA co-treatments with DXR for 24 h detected by flow cytometer; (b) percentages of live, early apoptosis, and late apoptosis/necrosis cells in response to the treatments (mean \pm S.E.) ($n = 3$); * $p < 0.05$ significantly different from the medium control; # $p < 0.05$ significantly different from the DXR.

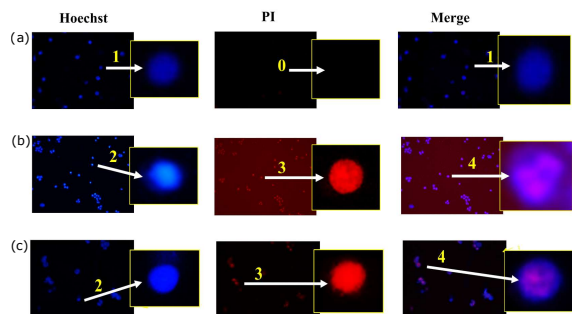


Fig. 5 Representative photos of Hoechst 33258/propidium iodide double staining of treated MCF-7 breast cancer cells: (a) the MEM medium control; (b) the 125 µg/ml 10-H2DA co-treated with 0.54 µg/ml DXR; (c) the DXR alone. Arrows indicate: (0) no dead cell; (1) viable cells with normal nuclei; (2) live cells with apoptotic nuclei; (3) dead cells; and (4) dead cells with apoptotic nuclei.

Nuclear morphological changes detected by Hoechst33258/propidium iodide double staining

The results of nuclear morphological changes using Hoechst33258/propidium iodide double staining showed that the 125 µg/ml 10-H2DA co-treatment with DXR and the DXR treatment alone caused a number of dead cells with apoptotic nuclei, whereas the MEM medium treatment showed regular MCF-7 treated cells without apoptotic nuclei, as shown in Fig. 5a, 5b, and 5c.

Effects on HO-1, NRF2, c-MYC, hTERT, p53, BAX, and BCL2 protein expression levels

The 10-H2DA (1.25-125 µg/ml) co-treatment with DXR decreased the c-MYC, the BCL2, and the hTERT levels while increasing the BAX, the p53, the NRF2, and the HO-1 levels in a relatively dose-dependent manner (Fig. 6a and 6b). As reported in previous studies [14, 15], protein expression levels were better expressed in a relationship with BAX, such as c-MYC/BAX, hTERT/BAX, NRF-2/BAX, and p53/BAX, and protein expressions from live cells versus dead cells were similar to the rheostat ratio, BCL2/BAX [16]. Moreover, BAX could serve as an internal control for comparing different levels of these regulatory proteins.

Evaluation of the regulatory protein values over BAX (Fig. 6c) demonstrated that the 125 µg/ml 10-H2DA co-treatment effectively inhibited cancer cell proliferation via the extensive suppression of the oncoprotein c-MYC/BAX (0.07-fold) and the high activation of the tumor suppressor p53/BAX (12.7-fold), compared with the MEM medium control. In addition, the 125 µg/ml 10-H2DA co-treatment caused a maximum decrease in the BCL2/BAX (0.2-fold) and a high decrease in the hTERT/BAX (0.3-fold), indicating strong induction of cell apoptosis and short-

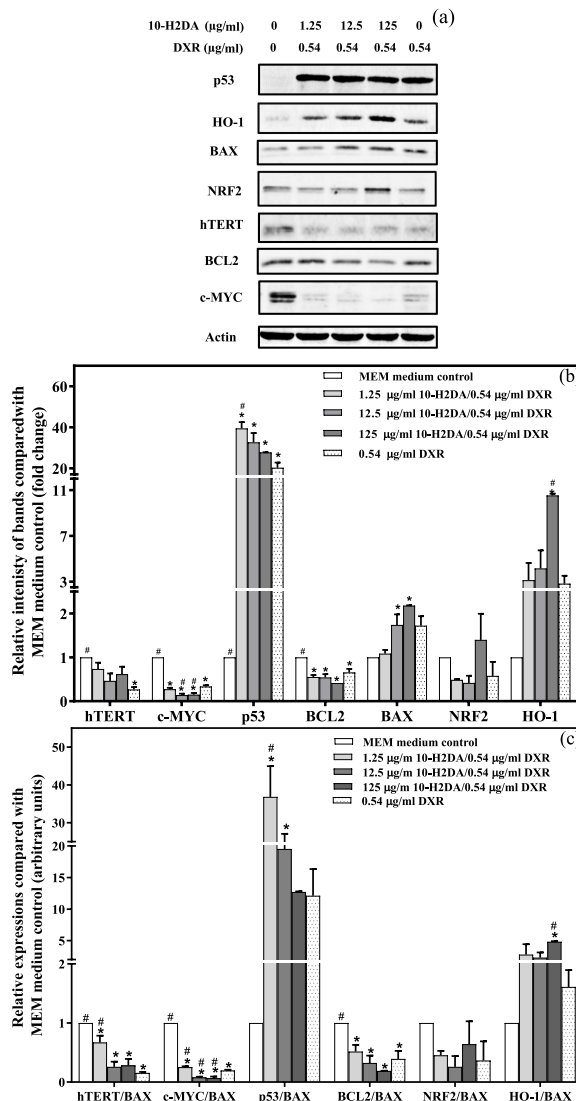


Fig. 6 (a) Representative Western blot analyses; (b) relative protein expression levels of various concentrations of the 10-H2DA co-treatments with DXR, compared with the MEM medium control (mean ± SE); * *p* < 0.05 significantly different from the MEM medium control; # *p* < 0.05 significantly different from the DXR; (c) relative protein expression levels over BAX of 10-H2DA co-treatments with the DXR, compared with the medium control (*n* = 3).

ened lifespan. It highly activated the HO-1/BAX (4.8-fold) and the p53/BAX (12.7-fold) while depleting the NRF-2/BAX (0.6-fold), suggesting induction of cell death via ferroptosis. Ferroptosis is a new cell death pathway mediated by iron and lipid peroxidation that produces reactive oxygen species (ROS) contributing to anticancer activity [16]. Activation of HO-1 enhanced heme degradation into biliverdin and ferrous ion, which induced the production of ROS that acted

as a ferroptosis activator [18, 19]. The increased p53 inhibited cystine uptake and decreased glutathione synthesis; then the ROS were produced, leading to ferroptosis and tumor suppression [20, 21]. The decreased NRF2 suppressed cells' anti-oxidant capacity; hence the ROS were induced and ferroptosis occurred [22, 23]. Therefore, the 125 $\mu\text{g/ml}$ 10-H2DA co-treatment increased the HO-1/BAX and the p53/BAX while decreasing the NRF2/BAX, possibly leading to ROS production, cell ferroptosis, and inhibition of cancer cell proliferation.

Additionally, the activation of HO-1/BAX and the suppression of NRF-2/BAX could limit chemoresistance and tumor invasion or metastasis. Reports revealed that activation of HO-1 in breast cancer cell lines reversed the chemotherapy resistant cancer cells into sensitized cells [24, 25], and it also inhibited cancer cell invasion and metastasis [18]. The NRF2 inhibition was found to reverse the cisplatin-resistant head and neck cancer cells to artesunate-induced ferroptosis [26]. The blockage of the NRF2 suppressed matrix metalloproteinase and, subsequently, inhibited cancer cell migration and invasion [27]. Our findings indicated that the 125 $\mu\text{g/ml}$ 10-H2DA co-treatment effectively inhibited cancer cell proliferation via suppression of the oncoprotein cMYC/BAX and the induction of p53/BAX, leading to G0-G1/S cell cycle arrest, cell apoptosis, and shortened lifespan. In addition, it possibly increased cell ferroptosis, reversed chemoresistant to sensitized chemotherapy, and limited cell metastasis since our results showed the suppression of the NRF2/BAX and the activation of both the HO-1/BAX and the p53/BAX. However, further investigation is needed to verify these possibilities (induction of ferroptosis and limiting chemoresistance and metastasis).

The DXR alone decreased the c-MYC/BAX (0.2-fold), the hTERT/BAX (0.2-fold), the BCL2/BAX (0.4-fold), and the NRF2/BAX (0.3-fold) while increasing the p53/BAX (11.8-fold) and the HO-1/BAX (1.6-fold), compared with the MEM medium control. These results indicated that the DXR treatment alone was less effective in inhibiting the MCF-7 cell growth than the 125 $\mu\text{g/ml}$ 10-H2DA co-treatment. However, it enhanced cell growth (higher level of the c-MYC/BAX) and lessened cell apoptosis (higher level of the BCL2/BAX and lower level of the p53/BAX).

The 1.25 $\mu\text{g/ml}$ 10-H2DA cotreatment decreased the c-MYC/BAX (0.3-fold), the hTERT/BAX (0.6-fold), the BCL2/BAX (0.5-fold), and the NRF2/BAX (0.5-fold) while increasing the p53/BAX (36.5-fold) and the HO-1/BAX (2.9-fold), compared with the MEM medium control. In comparison to the DXR treatment alone, the 1.25 $\mu\text{g/ml}$ 10-H2DA co-treatment was better at enhancing MCF-7 cell growth via antagonistic effect against the DXR treatment alone. This antagonistic effect might be a result of many possible reasons.

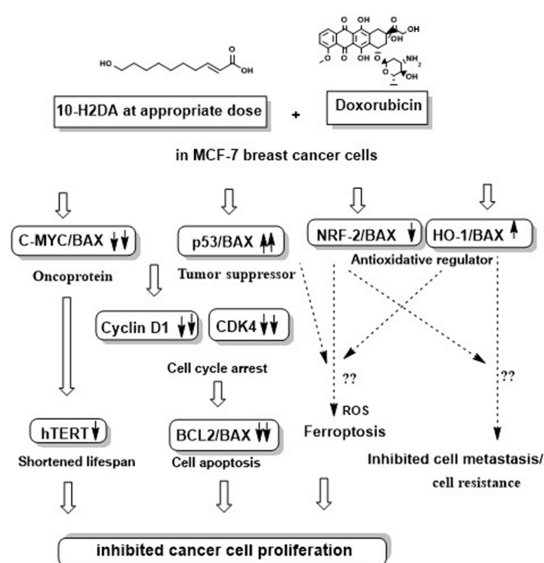


Fig. 7 Proposed underlying molecular mechanisms of antiproliferative effects induced by the 10-H2DA co-treatment with the DXR against MCF-7 breast cancer cells.

Firstly, the low dose co-treatment could activate the oncoprotein c-MYC/BAX (0.3-fold), and the higher doses could activate the lifespan extension controller hTERT/BAX (0.6-fold). These activations might overcome the p53/BAX activation, resulting in less cell apoptosis (higher level of the BCL2/BAX, 0.5-fold). Secondly, the 10-H2DA co-treatment activated the NRF-2/BAX and the HO-1/BAX at higher doses which might also inactivate some DXR's activities. Therefore, the increases in the c-MYC/BAX and the hTERT/BAX combined with the BCL2/BAX, the NRF2/BAX, and the HO-1/BAX by the 1.25 $\mu\text{g/ml}$ 10-H2DA co-treatment may play a major role in enhancing the MCF-7 cell proliferation and antagonize the inhibitory activity induced by the DXR treatment alone.

Taken all together, the 125 $\mu\text{g/ml}$ 10-H2DA co-treatment demonstrated the most effective antiproliferation against the MCF-7 breast cancer cells, followed by the DXR treatment alone. The low dose of 1.25 $\mu\text{g/ml}$ 10-H2DA co-treatment revealed antagonistic effect against the DXR treatment alone. The underlying mechanisms induced by the 125 $\mu\text{g/ml}$ 10-H2DA co-treated with the DXR in MCF-7 breast cancer cells were mainly the c-MYC/BAX suppression and the p53/BAX activation. The two mechanisms could lead to cell cycle arrest (decreased CDK4 and cyclin D1), cell apoptosis (decreased BCL2/BAX), and limited lifespan extension (decreased hTERT/BAX). The 125 $\mu\text{g/ml}$ 10-H2DA co-treatment also increased the HO-1/BAX and the p53/BAX, and decreased the NRF2/BAX, probably by promoting cell death via ferroptosis and potentially

limiting chemoresistance and tumor metastasis. The proposed inhibitory mechanisms of the 125 µg/ml 10-H2DA co-treatment are summarized in Fig. 7.

CONCLUSION

Treatment of the 10-H2DA in adjunct to the DXR at proper dose is a promising candidate for breast cancer treatment. Further *in vivo* mechanistic studies are necessary to validate its benefits.

Acknowledgements: The authors gratefully appreciate Prof. Dr. William W. Au for his criticism and valuable advice. Special thanks to Debra Kim Liwiski and Michael Everts for their careful assistance in editing this paper. The authors gratefully acknowledge the financial support provided by Thammasat University Research Fund under the TU Research Scholar, Contract No. TUFT 16/2562, Thailand.

REFERENCES

1. Ferlay J, Ervik M, Lam F, Colombet M, Mery L, Piñeros M, Znaor A, Soerjomataram I, Bray F (2020) *Global Cancer Observatory: Cancer Today*. International Agency for Research on Cancer, Lyon, France. Available at: <https://gco.iarc.fr/today>.
2. Palliyage GH, Ghosh R, Rojanasakul Y (2020) Cancer chemoresistance and therapeutic strategies targeting tumor microenvironment. *ScienceAsia* **46**, 639–649.
3. Kalyanaraman B (2020) Teaching the basics of the mechanism of doxorubicin-induced cardiotoxicity: Have we been barking up the wrong tree? *Redox Biol* **29**, ID 101394.
4. Tan ML, Choong PF, Dass CR (2009) Review: doxorubicin delivery systems based on chitosan for cancer therapy. *J Pharm Pharmacol* **61**, 131–142.
5. Dasari S, Tchounwou PB (2014) Cisplatin in cancer therapy: molecular mechanisms of action. *Eur J Pharmacol* **740**, 364–378.
6. Delmas D, Xiao J, Vejux A, Aires V (2020) Silymarin and cancer: a dual strategy in both in chemoprevention and chemosensitivity. *Molecules* **25**, ID 2009.
7. Honda Y, Araki Y, Hata T, Ichihara K, Ito M, Tanaka M, Honda S (2015) 10-hydroxy-2-decenoic acid, the major lipid component of royal jelly, extends the lifespan of *Caenorhabditis elegans* through dietary restriction and target of rapamycin signaling. *J Aging Res* **2015**, ID 425261.
8. Chen YF, Wang K, Zhang YZ, Zheng YE, Hu FL (2016) *In vitro* anti-inflammatory effects of three fatty acids from royal jelly. *Mediators Inflamm* **2016**, ID 3583684.
9. Ratanavalachai T, Wongchai V (2002) Antibacterial activity of intact royal jelly, its lipid extract and its defatted extract. *Thammasat Int J Sci Tech* **7**, 5–12.
10. Townsend GF, Morgan JF, Tolnai S, Hazlett B, Morton HJ, Shuel RW (1960) Studies on the *in vitro* anti-tumor activity of fatty acids. I. 10-hydroxy-2-decenoic acid from royal jelly. *Cancer Res* **20**, 503–510.
11. Bincoletto C, Eberlin S, Figueiredo CA, Luengo MB, Queiroz ML (2005) Effects produced by royal jelly on haematopoiesis: relation with host resistance against Ehrlich ascites tumour challenge. *Int Immunopharmacol* **5**, 679–688.
12. Pengpanich S, Srisupabh D, Tanechpongthamb WU (2019) Potential role of royal jelly and 10-hydroxy-2-decenoic acid as metastasis inhibitors in triple-negative breast cancer cells. *J Med Assoc Thai* **102**(S6), 17–24.
13. Jenkhetkan W, Itharat A, Kongkham S, Ruangnoo S, Ratanavalachai T (2021) Antiproliferative and cytotoxic efficacy of 10-hydroxy-2-decenoic acid, compared to doxorubicin, on MCF-7 breast cancer cells. *Trends Sci* **18**, ID 21.
14. Jenkhetkan W, Thitiourul S, Jansom C, Ratanavalachai T (2017) Molecular and cytogenetic effects of Thai royal jelly: modulation through c-MYC, h-TERT, NRF2, HO-1, BCL2, BAX and cyclins in human lymphocytes *in vitro*. *Mutagenesis* **32**, 525–531.
15. Jenkhetkan W, Thitiourul S, Jansom C, Ratanavalachai T (2018) Genoprotective Effects of Thai royal jelly against doxorubicin in human lymphocytes *in vitro*. *Nat Prod Commun* **13**, 79–84.
16. Korsmeyer SJ, Shutter JR, Veis DJ, Merry DE, Oltvai ZN (1993) Bcl-2/Bax: a rheostat that regulates an anti-oxidant pathway and cell death. *Semin Cancer Biol* **4**, 327–332.
17. Wang SJ, Ou Y, Jiang L, Gu W (2016) Ferroptosis: A missing puzzle piece in the p53 blueprint? *Mol Cell Oncol* **3**, e1046581.
18. Gandini NA, Alonso EN, Fermento ME, Mascaro M, Abba MC, Colo GP, Aevalo J, Ferronato MJ, et al (2019) Heme oxygenase-1 has an antitumor role in breast cancer. *Antioxid Redox Signal* **30**, 2030–2049.
19. Chiang SK, Chen SE, Chang LC (2018) A dual role of heme oxygenase-1 in cancer cells. *Int J Mol Sci* **20**, ID 39.
20. Jiang L, Kon N, Li T, Wang SJ, Su T, Hibshoosh H, Baer R, Gu W (2015) Ferroptosis as a p53-mediated activity during tumour suppression. *Nature* **520**, 57–62.
21. Kang R, Kroemer G, Tang D (2019) The tumor suppressor protein p53 and the ferroptosis network. *Free Radic Biol Med* **133**, 162–168.
22. Dixon SJ, Lemberg KM, Lamprecht MR, Skouta R, Zitsev EM, Gleason CE, Patel DN, Bauer AJ, et al (2012) Ferroptosis: an iron-dependent form of nonapoptotic cell death. *Cell* **149**, 1060–1072.
23. Dodson M, Castro-Portuguez R, Zhang DD (2019) NRF2 plays a critical role in mitigating lipid peroxidation and ferroptosis. *Redox Biol* **23**, 101–107.
24. Shin D, Kim EH, Lee J, Roh JL (2018) Nrf2 inhibition reverses resistance to GPX4 inhibitor-induced ferroptosis in head and neck cancer. *Free Rad Biol Med* **129**, 454–462.
25. Jaramillo MC, Zhang DD (2013) The emerging role of the Nrf2-Keap1 signaling pathway in cancer. *Genes Dev* **27**, 2179–2191.
26. Roh JL, Kim EH, Jang H, Shin D (2017) Nrf2 inhibition reverses the resistance of cisplatin-resistant head and neck cancer cells to artesunate-induced ferroptosis. *Redox Biol* **11**, 254–262.
27. Shen H, Yang Y, Xia S, Rao B, Zhang J, Wang J (2014) Blockage of Nrf2 suppresses the migration and invasion of esophageal squamous cell carcinoma cells in hypoxic microenvironment. *Dis Esophagus* **27**, 685–692.